Available online at www.sciencedirect.com

SciVerse ScienceDirect

Journal of the European Ceramic Society 32 (2012) 381–388

www.elsevier.com/locate/jeurceramsoc

Structural and optical properties of Tm:Y_2O_3 transparent ceramic with La_2O_3, ZrO_2 as composite sintering aid

Qing Yi [a,b], Shengming Zhou [a,*], Hao Teng [a], Hui Lin [a], Xiaorui Hou [a,b], Tingting Jia [a,b]

[a] *Key Laboratory of Materials for High Power Laser, Shanghai Institute of Optics and Fine Mechanics, Chinese Academy of Sciences, P.O. Box 800-211, Shanghai 201800, China*

[b] *Graduate School of Chinese Academy of Sciences, Beijing 100049, China*

Received 19 June 2011; received in revised form 5 September 2011; accepted 17 September 2011

Available online 12 October 2011

Abstract

The paper reports the use of La_2O_3 and ZrO_2 co-doping as a composite sintering aid for the fabrication of Tm:Y_2O_3 transparent ceramics. Two groups of experiments were conducted for investigating the influences of composite sintering aids on the microstructures and the optical properties of Tm:Y_2O_3 transparent ceramics in contrast to single La^{3+} and single Zr^{4+} doped Tm:Y_2O_3. Samples with composite sintering aids could realize fine microstructures and good optical properties at relatively low sintering temperatures. Grain sizes around 10 μm and transmittances close to theoretical value at wavelength of 2 μm were achieved for the 9 at.% La^{3+}, 3 at.% Zr^{4+} co-doped samples sintered at 1500–1600 °C. The influences of the composite sintering aids on the emission intensities and the phonon energies of Tm:Y_2O_3 ceramics were also investigated.

Keywords: Y_2O_3; Transparent ceramic; Sintering; Grain size; Optical properties

1. Introduction

Thulium based lasers around 2 μm are contributing factors in the developments of medical and remote sensing instrument based on their eye safe properties and high atmospheric transmittances.[1–4] Traditional host materials for Tm^{3+} active ion are YAG single crystals,[5–7] which have been highly developed because of their easy fabrications and profound investigations. Some other Tm^{3+} doped crystals such as vanadates[8] and YAP single crystals have been investigated.[9,10] However, vanadates demonstrate a laser performance that deteriorates greatly with increasing temperatures.[8] YAP single crystals exhibit a good laser performance, but their twinning, coloration and slightly inferior thermomechanical properties constrict the application.[9]

In recent years, Y_2O_3 has been considered as an alternative to traditional laser host materials. Y_2O_3 possesses higher thermal conductivitiy (27 W/m K for un-doped Y_2O_3) and lower phonon energies[11] comparing with YAG, which can ensure the stable laser operations. In addition, the broad transparent region from UV to IR makes Y_2O_3 suitable for laser oscillation. A few papers reported the crystal growth of Y_2O_3,[11,12] but the high melting point and the high-temperature phase transition of Y_2O_3 make the growth of Y_2O_3 single crystal difficult and seriously constrict the sizes of as-obtained crystals.

Since the first demonstration of Nd^{3+}:YAG ceramic laser by Ikesue et al.,[13] ceramic laser materials have attracted great attention for their low costs, easy productions and good optical properties. More importantly, the fabrication method of laser ceramics makes the high melting point sesquioxides such as Y_2O_3 possible to be used as laser media, which is hard to realize through conventional single crystal growth methods.

In this paper we present Tm^{3+} doped Y_2O_3 transparent ceramics with good optical properties. Sintering aids are pivotal factors for high grade transparent ceramics. Hou et al. introduced a sintering method involving ZrO_2 as the sintering aid,[14] which successfully led to high grade Y_2O_3 ceramics with small grain sizes. But this method needs high temperature sintering and long sintering period that cost too much energy. Others reported a sintering method with La_2O_3 as sintering aid leading to high transmittance Y_2O_3 ceramics by relatively

* Corresponding author at: Key Laboratory of Materials for High Power Laser, Shanghai Institute of Optics and Fine Mechanics, Chinese Academy of Sciences, P.O. Box 800-211, Shanghai 201800, China. Tel.: +86 21 69918482; fax: +86 21 69918482.

E-mail address: zhousm@siom.ac.cn (S. Zhou).

0955-2219/$ – see front matter.
doi:10.1016/j.jeurceramsoc.2011.09.015

Table 1
Sintering aid doping concentrations of the eight samples corresponding to different sintering temperatures.

Experimental group	Sample number	Sintering temperature/°C	Concentration of Zr^{4+} (value of x)	Concentration of La^{3+} (value of y)
Group 1	1	1500	0	0.09
	2	1500	0.03	0.09
	3	1600	0	0.09
	4	1600	0.03	0.09
Group 2	5	1700	0.03	0
	6	1700	0.03	0.03
	7	1800	0.03	0
	8	1800	0.03	0.03

low temperature sintering,[15] but the grain sizes were abnormally big and distributed in a wide range. For the first time we used La_2O_3, ZrO_2 co-doped as composite sintering aids, which led to good quality transparent ceramics with small grain sizes by sintering at relatively low temperatures. The optical properties of the La_2O_3, ZrO_2 co-doped Tm:Y_2O_3 transparent ceramics were investigated comparing with the single La_2O_3 and the single ZrO_2 doped Tm:Y_2O_3 sintered at the same condition.

2. Experiment

2.1. Ceramic fabrication

High purity commercial powders of Y_2O_3(99.99%), Tm_2O_3(99.99%), La_2O_3(99.99%), ZrO_2(99.99%) were used as the starting materials. The powders were weighed according to the stoichiometry of $(Zr_xLa_yTm_{0.03}Y_{0.97-x-y})_2O_3$ (listed in Table 1) with a fixed Tm^{3+} concentration of 3 at.%, and then ball milled in alcohol for 20 h. The obtained slurries were dried and then grinded with a pestle. The mixed powders were sieved through a 200 mesh screen. After that the powders were dry pressed in a stainless steel mold into discs with 15 mm in diameter and 3 mm in height under a low pressure. And then, the discs were cold-isostatic-pressed under 250 MPa. The pressed discs were calcined at 600–1000 °C for 2 h. Eventually the transparent ceramics were obtained after vacuum sintering at 1500–1800 °C for 20 h with a vacuum degree of 1×10^{-3} Pa. The different sintering temperatures attached to varied x, y values are listed in Table 1.

2.2. Characterization

The as-obtained ceramics were polished on both sides for measurements. The optical transmittances were obtained by a JASCO V-900 UV/VIS/NIR spectrophotometer. The emission spectra and fluorescence decay curves were recorded by a FLS920 fluorescence spectrophotometer (Edinburgh Instruments) with an excitation at 808 nm. The polished discs were etched in H_3PO_4 at 80 °C for 3 min for the observation of the microstructures. The microstructures were observed using a JSM 6360-LA scanning electron microscopy. Raman spectra were obtained using a Renishaw inVia Raman Microscope with an excitation at 514 nm for the determining of phonon energies.

3. Results and discussion

3.1. Densification and microstructure

We compared the La_2O_3, ZrO_2 co-doped Tm:Y_2O_3 samples with single La_2O_3 doped samples in group 1 and single ZrO_2 doped samples in group 2. In group 1, the concentrations of La^{3+} for all samples were fixed at 9 at.% and the sintering temperatures were in the range of 1500–1600 °C according to Ref. 15. The La^{3+} ions affect the sintering process by distorting the lattice, which cannot be achieved by a low doping concentration. And thus a high doping of 9 at.% was chosen. For comparison, the co-doped samples have an additional Zr^{4+} doping of 3 at.%. In group 2, the doping concentrations of Zr^{4+} for all samples were fixed at 3 at.% and sintering temperatures were in the range of 1700–1800 °C. The Zr^{4+} concentration and the temperatures we chose are empirical data and the details can be found in our previous papers.[14,16,17] For comparison, the co-doped samples have an additional La^{3+} doping of 3 at.%. The SEM photographs of the eight samples are shown in Figs. 1 and 2. The XRD patterns are shown in Fig. 3.

As we can see in Fig. 3, the XRD patterns of both the single doped and the co-doped ones match the standard cubic Y_2O_3 phase with a space group of $Ia{-}3$ perfectly. No extra peaks are found. It means that no secondary phase was formed in during the sintering.

The average grain sizes for samples 1–4 in group 1 were 69.1 μm, 9.6 μm, 78.5 μm, 10.1 μm, respectively, and the average grain sizes for samples 5–8 in group 2 were 24.9 μm, 38.3 μm, 32.1 μm, 45.8 μm, respectively. The average grain sizes were gained by multiplying the average intercept grain sizes with 1.56.[18] The average intercept grain sizes were obtained with the grain size calculation software attached to the SEM by calculating more than 200 grains. The grain sizes of the single La^{3+} doped samples (sample 1 and sample 3) were much larger than those of the single Zr^{4+} doped samples (sample 5 and sample 7) although the sintering temperatures of the single La^{3+} doped samples were lower than those of the single Zr^{4+} doped samples. This indicated that the La^{3+} ions enhanced the mobility of grain boundary while the Zr^{4+} ions strongly suppressed

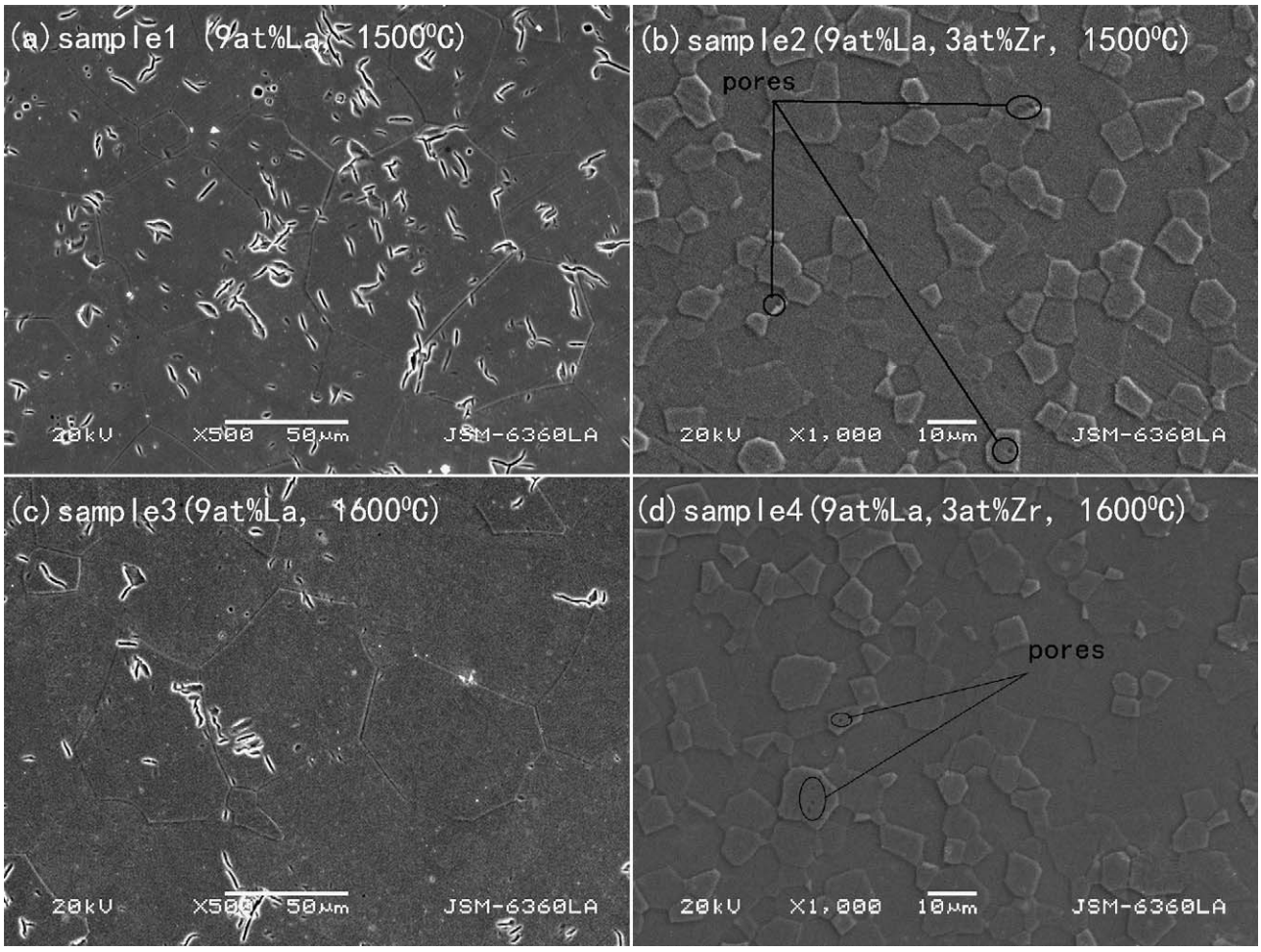

Fig. 1. SEM morphology of the chemistry-etched polished samples in experimental group 1: sample 1 (a), sample 2 (b), sample 3 (c), and sample 4 (d).

the migration of grain boundary, coinciding with the published literatures.[14,17,19,20–23] Considering the Y_2O_3 structure with one fourth of anion sites vacant,[24] the O^{2-} ions diffuse much faster than Y^{3+} ions. Moreover, as profoundly investigated,[23,25] the diffusion of Y^{3+} interstitial is ascertained to be the controlling step of sintering process in Y_2O_3 ceramic rather than Y^{3+} vacancy. In our experiment, the doping of La^{3+} could induce a distortion of the lattice or a modulation of phonon vibration spectra because of a larger radius (1.061 Å) than Y^{3+} ion (0.9 Å), which led to a faster diffusion of the Y^{3+} interstitial.[23] Thus the doping of La^{3+} inevitably led to a higher mobility of grain boundary. On the contrast, the doping of Zr^{4+} induced a decrease of O^{2-} vacancy concentration because of charge compensation. The Y^{3+} interstitial concentration and the O^{2-} vacancy concentration demonstrate a positive relationship between each other in Y_2O_3 which is presented in formula (1).[23] Therefore, the doping of Zr^{4+} led to a lower concentration of Y^{3+} interstitial, and hence a lower mobility of grain boundary in Y_2O_3 ceramic.

$$[Y_i^{\cdot\cdot\cdot}] = [V_{\ddot{O}}] \left(\frac{K_F}{K_S^{0.5}}\right) \exp\left[-\frac{\Delta G_F - \Delta G_S/2}{\kappa T}\right] \quad (1)$$

Formula (1) was deduced from a combination of Schottky defect and Frenkel defect in Y_2O_3 by Chen and Chen[23] and confirmed by other scientists,[17,26] where the K_F and K_S are the preexponential, temperature-independent factors of the reaction constants of Frenkel defect reaction and Schottky defect reaction in Y_2O_3, respectively, ΔG_F and ΔG_S are the Gibbs energy of the Frenkel defect reaction and Schottky defect reaction in Y_2O_3, respectively.

In group 2, as shown in Fig. 2, the grain sizes in the co-doped samples were larger than those in the single Zr^{4+} doped samples with the same sintering condition, which again confirmed the accelerating mechanism of La^{3+} ions. Besides, the co-doped sample achieved a fine microstructure at the temperature of 1700 °C while the single Zr^{4+} doped samples achieved the same grade structure at the higher temperature of 1800 °C. The defective structures of sample 5 and sample 8 indicated the samples were undersintered and oversintered, respectively.

The samples of group 1 shown in Fig. 1 gave much more dramatic results. The single La^{3+} doped samples, sample 1 and sample 3, sintered at low temperatures demonstrated microstructures with abnormally huge, defective grains while the microstructures with pretty small, defect-free grains were obtained for the co-doped samples with 3 at.% extra Zr^{4+}

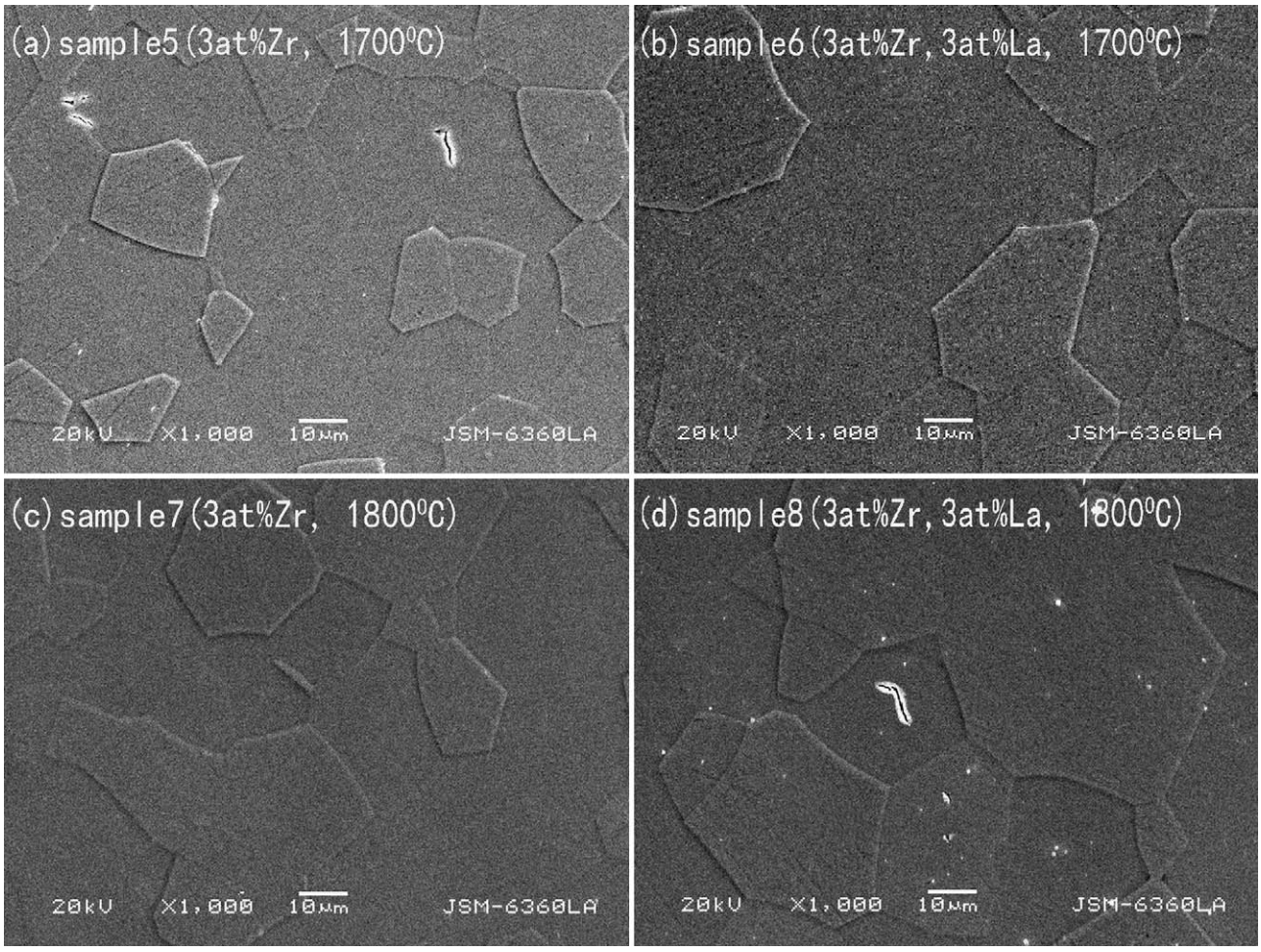

Fig. 2. SEM morphology of the chemistry-etched polished samples in experimental group 2: sample 5 (a), sample 6 (b), sample 7 (c), and sample 8 (d).

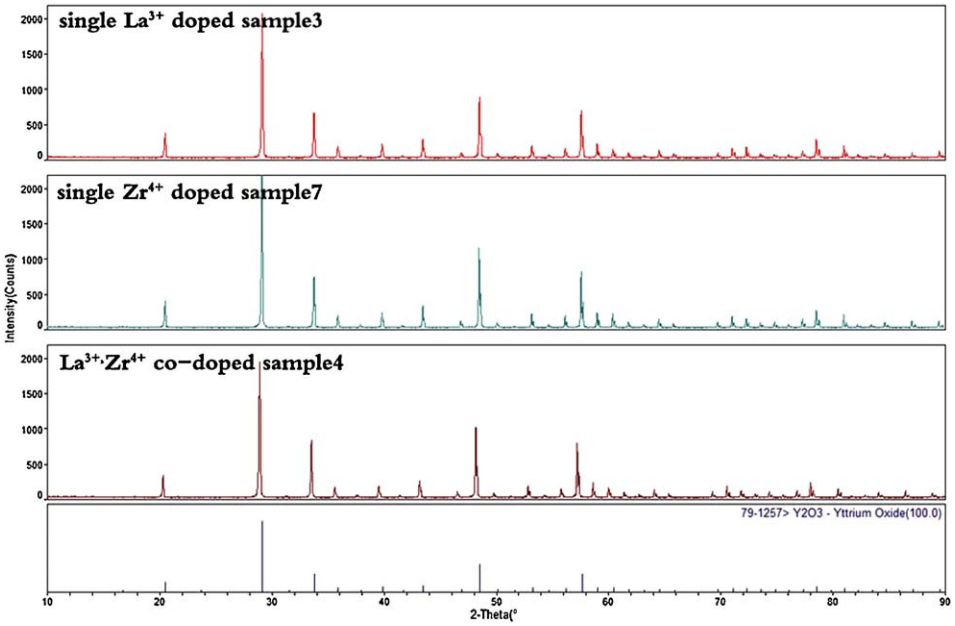

Fig. 3. XRD patterns of the Tm:Y_2O_3 ceramic samples.

sintering aid, named sample 2 and sample 4. The average grain sizes of samples 2 and 4 were 9.6 μm and 10.1 μm, respectively, which were the lowest in all the samples and lower than the data from the literatures for both single La^{3+} and single Zr^{4+} doped samples.[19,27] The literature 27 presents a two-step sintering method which successfully suppressed the grain size of La^{3+} doped Y_2O_3 to 25 μm, however, it is still larger than our data for samples 2 and 4. The small grain sizes in sample 2 and sample 4, especially in sample 2, were attributed to both the low sintering temperature and the small amount of Zr^{4+} which could suppress the grain boundary migration. As shown in Fig. 1b and d, samples 2 and 4 demonstrated pure, identical microstructures with only few small pores found inside the grains, as marked by circles in the micrographs. The doped Zr^{4+} and La^{3+} ions served as cooperation mechanisms in the sintering process. Given the low sintering temperatures, a small amount of Zr^{4+} ions could largely decelerate the mass transfer and hence suppressed the grain growth. A low mobility of grain boundary facilitated the pores to disappear from the grain boundaries, which was much easier than from inside the grains. The large amount of La^{3+} ions on the other hand accelerated the mass transfer in sintering process that accelerated the atoms to travel toward pores and enhanced the disappear velocity of pores. It seems that the Zr^{4+} and the La^{3+} have opposite influences on the mass transfer in sintering process. However, with proper doping concentrations and sintering conditions, the two different mechanisms complement each other and cooperate well, which can lead to the fine microstructures such as samples 2 and 4. The small grain sizes indicate that the Zr^{4+} ions have stronger effect on sintering than La^{3+} ions. The reason may be that the Zr^{4+} ion has a smaller radius (0.72 Å) comparing with Y^{3+} ion (0.9 Å), which can slightly moderate the lattice distortion induced by big La^{3+} ion (1.061 Å) and serves as a factor weakening the effect of La^{3+}. The microstructures of single La^{3+} doped samples 1 and 3 possessed a great number of pores. However, sample 3 was better than sample 1 due to the enhanced sintering temperature, with which we can anticipate that the single La^{3+} doped samples need even higher sintering temperatures to achieve a defect-free structure.

Both group 1 and group 2 showed that the co-doped samples can achieve fine microstructures at lower temperatures comparing with the single doped samples. Especially when the concentration of La^{3+} is high and the concentration of Zr^{4+} is low, as in the case of group 2, we can gain ceramics with pretty small grain sizes and fine microstructures at sintering temperature as low as 1500 °C. Small, uniform grain sizes can lead to good mechanical properties and high optical homogeneity which are essential for laser materials.

3.2. Optical properties

Figs. 3 and 4 show the transmittance spectra of group 1 and group 2, respectively. The absorption peaks around 680 nm, 800 nm, 1200 nm, 1630 nm were ascribed to the $^3H_6 \rightarrow {}^3F_2 + {}^3F_3$, $^3H_6 \rightarrow {}^3H_4$, $^3H_6 \rightarrow {}^3H_5$ and $^3H_6 \rightarrow {}^3F_4$ transitions in Tm^{3+} (inner-4f transitions), respectively. The $^3H_6 \rightarrow {}^3H_4$ transition was selected for excitation in emission

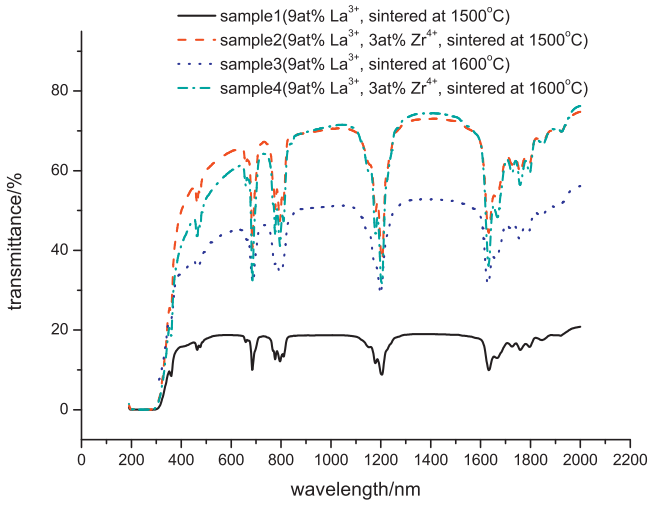

Fig. 4. Transmittance spectra of samples in experimental group 1.

spectrum measurements because of the good fitting with the commercial 808 nm diode laser.

Both the highest transmittances in two groups were achieved by the co-doped samples. In group 2, the highest transmittance was observed for sample 6, a 3 at.% Zr^{4+}, 3 at.% La^{3+} co-doped sample sintered at 1700 °C with a transmittance of 80.4% at 2 μm. Fig. 5 shows the picture of sample 6. The single Zr^{4+} doped sample sintered at the same temperature, named sample 5, had a transmittance of 76.9% at 2 μm, lower than the co-doped sample 6. After enhancing the sintering temperature to 1800 °C, the single Zr^{4+} doped sample, named sample 7, exhibited a higher transmittance in visible region comparing with single Zr^{4+} doped sample 5, which was consistent with the microstructure analyzed above. The transmittance of the co-doped sample deteriorated after enhancing the sintering temperature, as shown in sample 8, which indicated that the sample was oversintered.

In group 1, the co-doped sample 2 and sample 4 (Fig. 6a and b) were found to be similarly transparent with transmittances

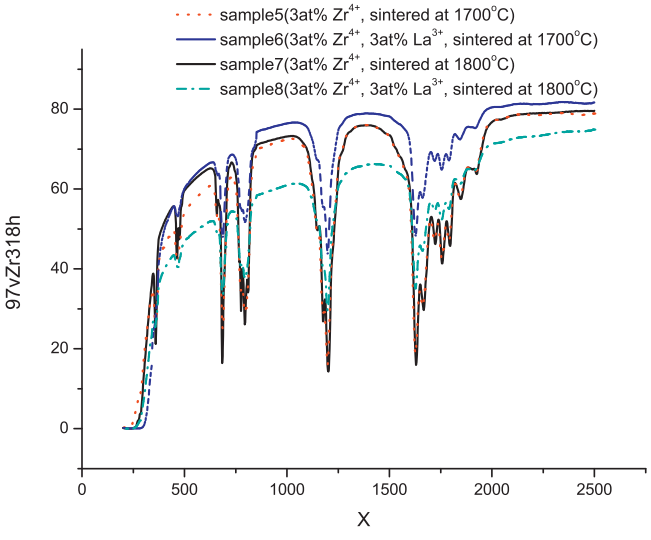

Fig. 5. Transmittance spectra of samples in experimental group 2.

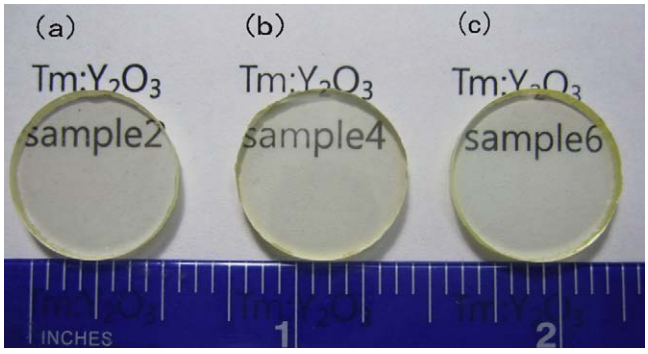

Fig. 6. Picture of the mirror polished sample 2 (a), sample 4 (b), and sample 6 (c).

of 76.2% and 74.8% at 2 μm, respectively, which were much higher than the single La^{3+} doped sample 1 (20.8%) and sample 3 (56.1%). However, the transmittances of sample 2 and sample 4 reached only 89.7% and 88% of the theoretical transmittance, respectively, which were still not high enough for laser application. The scattering came from the small pores found in the microstructures marked in Fig. 1b and d. This indicated that the co-doped samples in group 1 need further densification. A optimized scheme was performed by sintering a 9 at.% La^{3+}, 3 at.% Zr^{4+} sample at 1500 °C with a longer dwell time of 35 h, which was fixed to be 20 h in previous experiments, and a higher transmittance of 79.9% at 2 μm was achieved. The transmittance spectrum and the picture of this sample are shown in Fig. 6.

Fig. 7 shows the fluorescence spectra of selected samples. The samples had the same thickness of 2 mm and the spectra were recorded in the same measuring configuration. As obviously shown in the spectra, the intensities of the co-doped samples were much higher than those of the single La^{3+} and the single Zr^{4+} doped samples (threefold higher than the latter). Except the single La^{3+} doped sample 3, the other three samples had transmittances close to each other, which made the comparison of

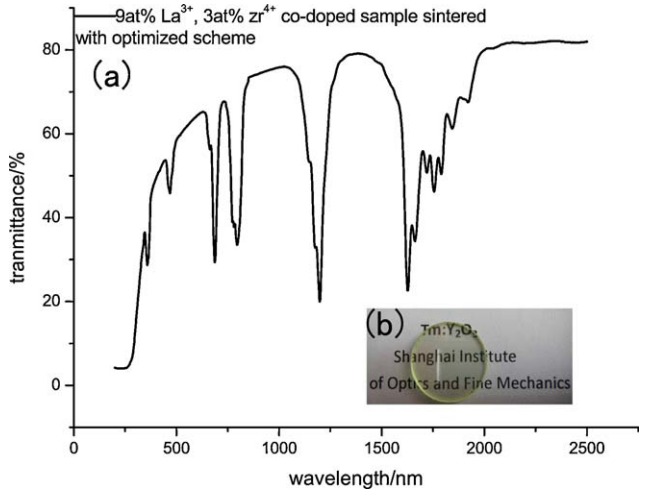

Fig. 7. Transmittance spectrum of a 9 at.% La^{3+}, 3 at.% Zr^{4+} co-doped sample sintered at 1500 °C for 35 h (a) and the picture of the mirror polished sample (b).

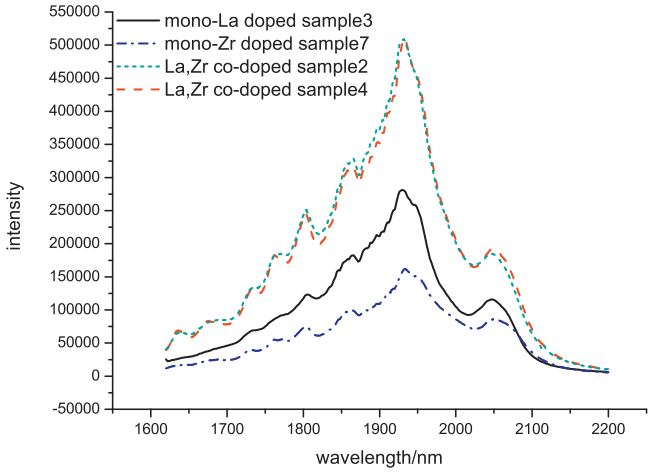

Fig. 8. Photoluminescence spectra of selected samples, excited by 808 nm diode laser.

photoluminescence intensities for the three samples valid. Thus we could draw a conclusion that the Y_2O_3 ceramics with La^{3+} in lattice could achieve higher photoluminescence intensity than those doped with Zr^{4+} only. It was hard to determine whether co-doped samples or single La^{3+} doped samples could achieve higher intensity. Because the single La^{3+} doped sample 3 used in this measurement had a much lower transmittance than both co-doped samples 2 and 4, which might decrease the detected luminescence intensity while measuring. Further investigation is undergoing.

As Fleuster and Buchal presented in the literature 28, the photoluminescence intensity is proportional to the life time τ of relative Stark level, $^3F_4$ of Tm^{3+} for this experiment, and the density of optically active ions ρ_{Tm}[28]

$$1 \propto \frac{\tau}{\tau_r}\rho_{Tm} \quad (2)$$

The life times of the co-doped sample 2, sample 4, single La^{3+} doped sample 3 and single Zr^{4+} doped sample 7 were measured to be 3.2 ms, 3.9 ms, 1.05 ms and 2.8 ms, respectively. This showed that the life times of the co-doped samples were much longer than the single doped samples. To the best of our knowledge, the best result we observed (3.9 ms) was longer than the best result observed in Tm:Y_2O_3 crystal, 3.08 ms for 5 at.% Tm^{3+} doping.[21] Thus the higher photoluminescence intensities of co-doped samples comparing with the single Zr^{4+} doped sample might result from the longer life time of co-doped samples.

3.3. Phonon energies

The phonon energy of Y_2O_3 is known to be much lower than YAG and YVO_4, which is beneficial for the photoluminescence applications.[11,29] In order to investigate the influence of sintering aids on the phonon energies of Y_2O_3 ceramic, selected samples together with a pure 6 at.% Tm:Y_2O_3 ceramic (an opaque sample without sintering aid) were measured by Raman spectra with an excitation at 514 nm, as shown in Fig. 8. The spectra were found to be almost identical with no peak shift among samples and the

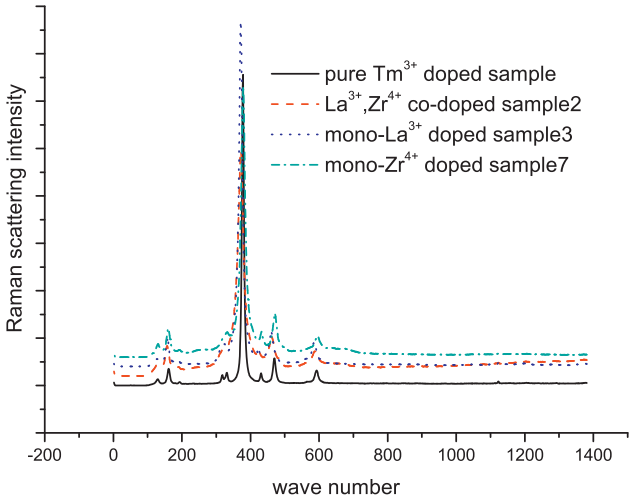

Fig. 9. Raman spectra of selected samples along with a pure Tm:Y_2O_3 ceramic without sintering aid.

largest phonon energy of all the samples was determined to be 587 cm^{-1}, while the phonon energy of YAG and YVO_4 can reach 857 cm^{-1} and 880 cm^{-1}, respectively, as reported (Fig. 9).[29]

4. Conclusion

In order to investigate the influence of La_2O_3, ZrO_2 composite sintering aid on the microstructure and the optical properties of the Tm:Y_2O_3 transparent ceramic comparing with single La^{3+} and single Zr^{4+} doped Tm:Y_2O_3, two experimental groups were conducted. We compared the co-doped samples with single La^{3+} doped samples and single Zr^{4+} doped samples in experimental group 1 and group 2, respectively.

Samples with composite sintering aid, especially with a high La^{3+} concentration and low Zr^{4+} concentration as in the case of group 1, could achieve fine microstructures and good optical properties at lower sintering temperature comparing with both single doped samples. Small average grain size around 10 μm was observed for samples in group 1, with a doping concentration of 9 at.% La^{3+} and 3 at.% Zr^{4+} and a sintering temperature in the range of 1500–1600 °C. The transmittance reached 79.93% at 2 μm while sintering at 1500 °C for 35 h.

The samples with La^{3+} in lattice exhibited higher photoluminescence intensity comparing with the single Zr^{4+} doped samples. The influence of the sintering aid on the phonon energy was negligible. All the samples exhibited similar Raman spectra without peak shift.

Acknowledgements

This work was supported by the Key Basic Research Project of Science and Technology Committee of Shanghai (No. 10JC1415700) and Natural Science Foundation of China (No. 60990311).

References

1. Wu CT, Ju YL, Zhou RL, Duan XM, Wang YZ. Achieving single-longitudinal-mode output about Tm:YAG laser at room temperature. *Laser Phys* 2011;**2**:372–5.
2. Rameix A, Borel C, Chambaz B, Ferrand B, Shepherd DP, Warburton TJ, et al. An efficient, diode-pumped, 2 μm Tm:YAG waveguide laser. *Opt Commun* 1997;**142**:239–43.
3. De Young RJ, Barnes NP. Profiling atmospheric water vapor using a fiber laser lidar system. *Appl Opt* 2010;**49**:562–7.
4. Henderson SW, Hale CP, Magee JR, Kavaya MJ, Huffaker AV. Eye-safe coherent laser-radar system at 2.1-μM using Tm,Ho-Yag lasers. *Opt Lett* 1991;**16**:773–5.
5. Pinto JF, Esterowitz L, Rosenblatt GH. Continuous-wave mode-locked 2-μM Tm–YAG laser. *Opt Lett* 1992;**17**:731–2.
6. Chang RSF, Hara H, Chaddha S, Sengupta S, Djeu N. Lasing performance of a Tm–Yag minirod grown by laser-heated pedestal growth technique. *IEEE Photon Tech Lett* 1990;**2**:695–6.
7. Stoneman RC, Esterowitz L. Efficient, broadly tunable laser-pumped Tm–YAG and Tm–YSGG CW lasers. *Opt Lett* 1990;**15**:486–8.
8. Lisiecki R, Solarz P, Dominiak-Dzik G, Ryba-Romanowski W, Lukasiewicz T. Effect of temperature on spectroscopic features relevant to laser performance of YVO_4:Tm^{3+}, $GdVO_4$:Tm^{3+}, and $LuVO_4$:Tm^{3+} crystals. *Opt Lett* 2010;**35**:3940–2.
9. Buryy OA, Sugak DY, Ubizskii SB, Izhnin II, Vakiv MM, et al. The comparative analysis and optimization of the free-running Tm^{3+}:YAP and Tm^{3+}:YAG microlasers. *Appl Phys B-Lasers Opt* 2007;**88**:433–42.
10. Li G, Yao BQ, Meng PB, Ju YL, Wang YZ. Efficient continuous wave and q-switched operation of a dual-end-pumped c-cut Tm:YAP laser. *Laser Phys* 2010;**20**:1871–6.
11. Mun JH, Jouini A, Novoselov A, Guyot Y, Yoshikawa A, et al. Growth and characterization of Tm-doped Y_2O_3 single crystals. *Opt Mater* 2007;**29**:1390–3.
12. Ermeneux FS, Sun Y, Cone RL, Equall RW, Hutcheson RL, et al. Efficient CW 2 mu m Tm^{3+}:Y_2O_3 laser. *Adv Solid-State Lasers* 1999;**26**:497–502.
13. Ikesue A, Kinoshita T, Kamata K, Yoshida K, Fabrication. Optical-properties of high-performance polycrystalline Nd–YAG ceramics for solid-state lasers. *J Am Ceram Soc* 1995;**78**:1033–40.
14. Hou XR, Zhou SM, Li YK, Li WJ. Effect of ZrO_2 on the sinterability and spectral properties of $(Yb_{0.05}Y_{0.95})_2O_3$ transparent ceramic. *Opt Mater* 2010;**32**:920–3.
15. Rhodes WH. Physical-properties of transparent La_2O_3-doped Y_2O_3. *J Met* 1981;**33**:A50.
16. Hou XR, Zhou SM, Li WJ, Li YK, Lin H, et al. Investigation of the spectroscopic properties of highly transparent Yb:$(Y_{0.97}Zr_{0.03})_2O_3$ ceramic. *Opt Mater* 2010;**32**:1435–40.
17. Hou XR, Zhou SM, Li WJ, Li YK. Study on the effect and mechanism of zirconia on the sinterability of yttria transparent ceramic. *J Eur Ceram Soc* 2010;**30**:3125–9.
18. Fullman RL. Measurement of particle size in opaque bodies. *Trans Am Inst Min Metal Pet Eng* 1953;**1970**:447–56.
19. Hou XR, Zhou SM, Jia TT, Lin H, Teng H. Structural, thermal and mechanical properties of transparent Yb:$(Y_{0.97}Zr_{0.03})_2O_3$ ceramic. *J Eur Ceram Soc* 2011;**31**:733–8.
20. Hou XR, Zhou SM, Jia TT, Lin H, Teng H. White light emission in Tm^{3+}/Er^{3+}/Yb^{3+} tri-doped Y_2O_3 transparent ceramic. *J Alloys Compd* 2011;**509**:2793–6.
21. Lu SZ, Zhang HJ, Yang QH, Xu J. Spectral properties of Er/Yb:$(Y_{0.9}La_{0.1})_2O_3$ and Er/Yb:Y_2O_3 transparent ceramics. In: *2009 Lasers & Electro-Optics & the Pacific Rim Conference on Lasers and Electro-Optics, vols. 1 and 2*. 2009. p. 804–5.
22. Yang QH, Xu J, Dou CG, Zhang HW, Ding J, Tang ZF. Effect of La_2O_3 doping on the spectroscopic properties of transparent Yb: Y_2O_3 laser ceramics. *Acta Phys Sin* 2007;**56**(7):3961–5.
23. Chen PL, Chen IW. Grain boundary mobility in Y_2O_3: defect mechanism and dopant effects. *J Am Ceram Soc* 1996;**79**:1801–9.
24. Gaboriaud RJ. Self-diffusion of yttrium in mono-crystalline yttrium-oxide – Y_2O_3. *J Solid State Chem* 1980;**35**:252–61.

25. Ando K, Oishi Y, Hase H, Kitazawa K. Oxygen self-diffusion in single-crystal Y_2O_3. *J Am Ceram Soc* 1983;**66**:C222–3.
26. Huang YH, Jiang DL, Zhang JX, Lin QL, Huang ZG. Sintering of transparent yttria ceramics in oxygen atmosphere. *J Am Ceram Soc* 2010;**93**:2964–7.
27. Huang YH, Jiang DL, Zhang JX, Lin QL. Fabrication of transparent lanthanum-doped yttria ceramics by combination of two-step sintering and vacuum sintering. *J Am Ceram Soc* 2009;**92**:2883–7.
28. Fleuster M, Buchal C, Snoeks E, Polman A. Optical structural-properties of MeV erbium-implanted $LiNbO_3$. *J Appl Phys* 1994;**75**: 173–80.
29. Yang WQ, Guo LH, Feng SY, Chen JK. Research on Raman spectra and energy transfer in Tm^{3+}, Ho^{3+} single and Co-doped YVO_4 crystals. *Spectrosc Spectr Anal* 2007;**27**:581–4.